Fragmentation of valence electronic states of CF+4 and SF+6 studied by threshold photoelectron–photoion coincidence spectroscopy

ARTICLE *in* CHEMICAL PHYSICS · AUGUST 1993

Impact Factor: 1.65 · DOI: 10.1016/0301-0104(93)80010-7

7 AUTHORS, INCLUDING:

Richard P Tuckett
University of Birmingham
162 PUBLICATIONS **2,057** CITATIONS

SEE PROFILE

Chemical Physics 174 (1993) 441–452
North-Holland

Fragmentation of valence electronic states of CF_4^+ and SF_6^+ studied by threshold photoelectron–photoion coincidence spectroscopy

J.C. Creasey, H.M. Jones, D.M. Smith, R.P. Tuckett
School of Chemistry, University of Birmingham, Edgbaston, Birmingham B15 2TT, UK

P.A. Hatherly [1], K. Codling
J.J. Thomson Physical Laboratory, University of Reading, Whiteknights, Reading RG6 2AF, UK

and

I. Powis
Department of Chemistry, University Park, Nottingham NG7 2RD, UK

Received 15 March 1993

Threshold photoelectron–photoion coincidence (TPEPICO) spectroscopy has been used to measure, state selectively, the decay pathways of all the valence states of CF_4^+ and SF_6^+ in the range 15–28 eV. Radiation in the vacuum UV from a synchrotron radiation source ionises the parent molecule, and the electrons and ions are detected by threshold electron analysis and time-of-flight mass spectroscopy, respectively. TPEPICO spectra are recorded continuously as a function of photon energy, allowing both threshold photoelectron spectra and yields of all the fragment ions to be obtained. Kinetic energy releases are measured at fixed photon energies with good time resolution. The results for the $\tilde{X}\ ^2T_1$, $\tilde{A}\ ^2T_2$ and $\tilde{B}\ ^2E$ states of CF_4^+ (all below the energy of He I radiation) confirm earlier measurements; results for the $\tilde{C}\ ^2T_2$ and $\tilde{D}\ ^2A_1$ states at 21.7 and 25.1 eV, respectively, are new. They confirm previous measurements that radiative decay from both states is an important process, and we have measured their state-selected fluorescence quantum yields. For SF_6^+, fluorescence does not occur from any of the excited valence states, and we have measured the fragmentation channels and branching ratios for all of the valence states.

1. Introduction

Coincidence techniques are now well established as a means to determine the decay dynamics of selected vibronic states of molecular ions. For single-ionisation events the most commonly used is the photoelectron–photoion coincidence (PEPICO) technique in which energy analysed photoelectrons are detected in coincidence with ions which have been mass-selected in a time-of-flight (TOF) spectrometer [1]. The majority of the early experiments used fixed frequency lines from gas discharge lamps (e.g. the He I line at 584 Å or 21.22 eV) as the excitation source with an electron energy analyser, i.e.

$$AB_n + h\nu \rightarrow (AB_n)^{+*} + e^- .$$

AB_n represents a general polyatomic molecule, and the asterisk an excited electronic state. The electron analyser is used to define the kinetic energy (KE) of the ejected electron, and thus the state of the ion AB_n^+. In such studies one is limited by the photon energy of the excitation source and the resolution of the electronic analyser, which is typically several tens of meV. With the availibility of tunable sources of vacuum UV radiation from dedicated synchrotrons and zero kinetic energy (threshold) electron analysers with high sensitivity and resolution, both problems can be circumvented. We have recently constructed a threshold photoelectron–photoion coincidence (TPEPICO) experiment which is attached

[1] To whom correspondence should be addressed.

to a VUV beam line at the Daresbury synchrotron source [2]. This paper describes the results obtained for fragmentation of the polyatomic ions CF_4^+ and SF_6^+.

The ground states of CF_4^+ and SF_6^+ are unusual in that they are repulsive states which fragment on a subpicosecond timescale by loss of a fluorine atom to $CF_3^+ + F$ and $SF_5^+ + F$, respectively [3]. This arises because the ionisation potentials (IPs) of the CF_3 and SF_5 radicals (9,2 and 10.0 eV [4,5]) are small compared to that of the stable molecules CF_4 and SF_6 (15.3 and 15.5 eV [6–8]). As a consequence the ground states of CF_4^+ and SF_6^+ lie *above* the respective thermodynamic dissociation energies to $CF_3^+ + F$ and $SF_5^+ + F$. A repulsive ground state implies that statistical theories (e.g. quasi-equilibrium theory [9]) cannot be used to determine the fragmentation pattern of the molecular ion for energies above threshold of fragment ion production. In previous work [10,11] we reported results from PEPICO experiments on CF_4^+ and SF_6^+ using tunable synchrotron radiation. However, the energy of the photoelectrons was not analysed, all electrons with energies up to 8 eV being collected with high efficiency. Ion yield curves and thresholds for fragment ion production were obtained. However, because the internal energy of the parent ion was not defined, the KE data for the fragment ions were only of limited value. It became clear that discrimination of the electron energy was necessary to select high-lying valence states of CF_4^+ and SF_6^+ in order to study their unimolecular decay dynamics. Threshold electron analysis is ideal in that it rejects energetic electrons produced from lower-lying states although, in addition to direct (Franck–Condon) ionisation, ions may also be formed by autoionisation via excited states of the neutral.

2. Experimental

Several methods are used to detect threshold electrons in coincidence experiments. In steradiancy analysis [12] electrons produced in the interaction region are accelerated into a field-free region consisting of a tube or collimated hole array with a large length/diameter ratio. The majority of the energetic electrons are rejected since they have non-axial velocities, hit the walls of the analyser and are lost. Low-energy or threshold electrons pass through the analyser parallel to the axis and reach the detector. Energetic electrons ejected parallel to the axis, however, are also detected, giving rise to a "high-energy tail" in the transmission function. They can be removed with a small dispersive post-analyser, but since steradiancy analysers do not focus the electrons, the overall collection efficiency is substantially reduced. In low extraction penetrating field analysis [13], low-energy electrons are extracted from the interaction region by a very weak electric field (a few meV/cm only). The configuration of the field is such that only threshold electrons come to a focus at the entrance to a small post-analyser, and the overall system has excellent resolution (≈ 3 meV) and high collection efficiency [13]. Problems arise when one tries to combine the penetrating field method with efficient detection of energetic ions, because a high extraction field in the interaction region is needed in a TOF mass spectrometer; the product of the electron and ion collection efficiencies determines the coincidence count rate in a PEPICO experiment.

Our threshold detector combines the best features of both analysers. It incorporates a cylindrical electrostatic lens designed with large chromatic aberrations, followed by a 127° post-analyser which rejects the hot electrons on axis [2]. Computer simulations show that the threshold analyser is capable both of high-resolution (≈ 3.5 meV half width) and high-collection efficiency (100% for zero energy electrons) even though the extraction field is as high as 20 V/cm. The ion detector consists of a two-stage acceleration region and a TOF drift tube configured to satisfy the space focusing condition [14]. This allows measurement of the KE release from a dissociative ion process whilst still retaining a high-collection efficiency. Vacuum UV radiation from a 1 m Seya monochromator attached to the Daresbury synchrotron source is admitted to the interaction region of the TPEPICO apparatus via a capillary, where it crosses an effusive spray of the sample gas. The base pressure of the chamber is 5×10^{-8} Torr, the maximum background pressure during an experiment is 1×10^{-4} Torr. The grating used in the Seya is blazed at 550 Å, and has a range of $\approx$400–800 Å with minimal second-order effects. Collimation of the photon beam is achieved with a thin wire coil coated with colloidal graphite inserted into the capillary [2]. The

photon flux is monitored by a sodium salicylate-photomultiplier tube combination, allowing flux normalisation of the data. Threshold electron and ion signals are fed into a time-to-digital converter (TDC, Le Croy 4208), the electrons providing the "start" pulse, the ions the "stop" pulse. Hence correlated electrons and ions from the same ionisation event are detected in delayed coincidence, providing a TPEPICO spectrum.

Three types of experiment can be performed. Firstly, the threshold photoelectron (or total ion) signal can be recorded as a function of photon wavelength. No threshold photoelectron spectrum (TPES) of either CF_4 or SF_6 in the valence ionisation region has been reported, and the main interest is how the spectra differ from the He I or He II photoelectron spectra. In the latter cases, direct (Franck–Condon) ionisation is the dominant mechanism for the production of energetic electrons. Threshold electrons, however, often form via resonant autoionisation, allowing ions to be created in states that cannot be accessed by direct ionisation. Secondly, a TPEPICO spectrum can be recorded at a fixed photon energy. Since signal from the parent ion is never observed with CF_4 or SF_6, only fragment ions are observed, often with substantial KE release. To obtain the kinetic energy release distribution (KERD) [15], accurate peak shapes are required and the TOF data are accumulated at a high time resolution of the TDC. Thirdly, a TPEPICO spectrum can be recorded as a function of photon wavelength. As in our earlier experiments [10,11], data accumulate as a 3D histogram of photon wavelength versus ion TOF versus coincidences, with the last variable being represented

Table 1
Energetics of dissociation channels of CF_4^+ and SF_6^+

Neutral/parent ion	Dissociation channel [a]	Dissociation energy (eV)	Adiabatic IP (eV) [b]
CF_4^+ $\tilde{D}\,^2A_1$			25.12
	$CF^+ + F + F_2$	22.1	
$\tilde{C}\,^2T_2$			21.70
	$CF_2^+ + F + F$	20.8	
	$CF_2^+ + F_2$	19.2	
$\tilde{B}\,^2E$			18.30
$\tilde{A}\,^2T_2$			17.10
$\tilde{X}\,^2T_1$			15.35
	$CF_3^+ + F$	14.7 [c]	
CF_4 $\tilde{X}\,^1A_1$			0
SF_6^+ $\tilde{F}\,^2A_{1g}$			26.83 [d]
	$SF^+ + F_2 + F_2 + F$	23.7	
$\tilde{E}\,^2T_{1u}$			22.3
	$SF_2^+ + F_2 + F_2$	19.7	
$\tilde{D}\,^2T_{2g}$			19.2
	$SF_3^+ + F + F + F$	19.0	
	$SF_4^+ + F + F$	18.4	
$\tilde{C}\,^2E_g$			18.0
	$SF_3^+ + F_2 + F$	17.4	
	$SF_4^+ + F_2$	16.8	
$\tilde{A}/\tilde{B}\,^2T_{1u}/^2T_{2u}$			16.7
$\tilde{X}\,^2T_{1g}$			15.5
	$SF_5^+ + F$	14.0	
SF_6 $\tilde{X}\,^1A_{1g}$			0

[a] Not all the dissociation channels involving CF^+, SF^+, SF_2^+, F_2^+ and F^+ are listed. The data to calculate these thermochemical energies are given in refs. [11,17].

[b] The second decimal point for the adiabatic IPs should be treated with caution.

[c] See section 5.1 of the text. [d] Ref. [18].

by colour. Data can be displayed either as a 3D histogram [16] or by taking cross-sectional cuts through it. Either the TOF spectrum can be shown at a particular photon energy, or more usefully the variation of a fragment ion yield with photon energy can be displayed. This latter method gives directly the thresholds for production of the fragment ions. Since all the ions produced in the TPEPICO spectrum are usually recorded in this "wavelength-scanning" mode, the threshold of the TDC is degraded. The energy resolution of all the TPES and TPEPICO spectra are limited by the monochromator, not by the threshold analyser, and typical values are 1–4 Å.

3. The energetics, dissociation channels and previous PEPICO studies of the electronic states of CF_4^+ and SF_6^+

3.1. CF_4

The electron configuration of the five highest occupied valence molecular orbitals (MOs) of CF_4 is $...(2a_1)^2(2t_2)^6(1e)^4(3t_2)^6(1t_1)^6$. Only the three highest orbitals are accessible with He I radiation. He I and He II photoelectron spectra were reported in the 1970s [6,7], and adiabatic ionisation potentials (IP) are given in table 1. The first two bands, corresponding to ionisation to the repulsive $\tilde{X}\ ^2T_1$ and $\tilde{A}\ ^2T_2$ states, show no vibrational structure. The third band ($(1e)^{-1} \rightarrow \tilde{B}\ ^2E$) shows a partially resolved progression in ν_1 (810 cm^{-1}) and possibly ν_2 (400 cm^{-1}), the latter arising from Jahn–Teller distortion of the $\tilde{B}$ state from T_d symmetry. The fourth band ($(2t_2)^{-1} \rightarrow \tilde{C}\ ^2T_2$) shows an extensive progression in ν_1 (645 cm^{-1}) peaking at $v_1 = 5$, whereas the fifth band ($(2a_1)^{-1} \rightarrow \tilde{D}\ ^2A_1$) has its strongest component at $v_1 = 0$ with only a weak progression in ν_1 (730 cm^{-1}). The energies of the ionic dissociation channels of CF_4 are also given in table 1 [17]. Since the ground state of CF_4^+ is repulsive, it fragments to $CF_3^+ + F$, as do the first two excited states. Although there has been some suggestion that the $\tilde{B}\ ^2E$ state fluoresces prior to dissociation [19,20], a photoion–fluorescence coincidence experiment has shown this to be incorrect [21]. This state probably undergoes rapid internal conversion into the $\tilde{A}$ state before fragmentation from the repulsive surface. The $\tilde{C}\ ^2T_2$ and $\tilde{D}\ ^2A_1$ states of CF_4^+ both show vibrational structure in their photoelectron bands, have lifetimes of 9 and 2 ns, respectively [17,22], and decay radiatively [17]. Given that several dissociation channels are energetically "open", this is a very surprising phenomenon. Internal conversion from these states to high-lying regions of lower electron states must therefore be slow ($< 10^8\ s^{-1}$) (see the following paper [23]). A discrete emission band arises from a transition between the $\tilde{D}$ and $\tilde{C}$ states [29], yielding improved vibrational constants. Continuous bands also arise from transitions to the lower $\tilde{X}$ and $\tilde{A}$ repulsive states (e.g. $\tilde{D}$–$\tilde{A}$, $\tilde{C}$–$\tilde{X}$) [25]. The fluorescence quantum yield of the $\tilde{C}$ state is estimated to be 0.5 ± 0.3 [10,17], and hence a competing non-radiative channel is operative. The quantum yield of the $\tilde{D}$ state has not been measured, but a lifetime as low as 2 ns would suggest that it too is substantially less than unity.

In our earlier PEPICO experiments [10] only CF_3^+ and CF_2^+ were observed, and yields were measured as a function of photon energy between 15 and 26 eV, i.e. from below the energy of the CF_4^+ $\tilde{X}$ state to above that of the $\tilde{D}$ state. Thresholds for CF_3^+ production were observed at the adiabatic IPs of the $\tilde{X}$ and $\tilde{A}$ states, but it was not possible to determine whether there were new thresholds at the $\tilde{B}$, $\tilde{C}$ or $\tilde{D}$ states because of the large CF_3^+ signal already present. Similarly, a threshold for CF_2^+ production was observed at the adiabatic IP of the $\tilde{C}$ state, but again the presence or absence of a new threshold at the $\tilde{D}$ state could not be determined. This, and the limited information that could be extracted from the KE releases, was a consequence of the lack of electron energy analysis.

3.2. SF_6

The electron configuration of the seven highest occupied valence MOs in SF_6 is $...(5a_{1g})^2(4t_{1u})^6 \cdot (1t_{2g})^6(3e_g)^4(1t_{2u})^6(5t_{1u})^6(1t_{1g})^6$. Table 1 shows the symmetries and adiabatic IPs of the valence of states SF_6^+ as measured by photoelectron and Rydberg spectroscopy [8,18]. Although there has been some disagreement in the assignment of the second photoelectron band, its assignment to an unresolved $(5t_{1u})^{-1}$ and $(1t_{2u})^{-1}$ doublet has recently been sup-

ported by theoretical calculations [26], and we assign this band to formation of SF_6^+ $\tilde{A}/\tilde{B}$ $^2T_{1u}/^2T_{2u}$. Vibrational structure has only been resolved in the fourth band (ionisation to $\tilde{D}$ $^2T_{2g}$) with a long progression observed in ν_1 (590 cm^{-1}). The energies of the ionic dissociation channels from SF_6 are given in table 1 [11]. Once again, we comment that the $SF_5^+ + F$ channel lies below the adiabatic IP of the ground state of SF_6^+, and several dissociation channels are "open" to the excited valence states of SF_6^+. A recent photoion–fluorescence coincidence experiment has shown that no states of SF_6^+ below the energy of He II radiation (40.8 eV) decay by photon emission [27], so all of these valence states decay non-radiatively by fragmentation.

In the earlier PEPICO experiments [11] ion yields for SF_5^+, SF_4^+ and SF_3^+ were measured between 15 and 28 eV, from below the energy of the SF_6^+ $\tilde{X}$ state to above that of the $\tilde{F}$ state. Thresholds for SF_5^+ production were observed at the adiabatic IP of the ground and first excited state pair of SF_6^+ ($\tilde{X}$ and $\tilde{A}/\tilde{B}$). SF_4^+ showed a threshold 0.5 eV above the adiabatic IP of the $\tilde{C}$ ^2E_g state of SF_6^+, and we tentatively assigned formation of SF_4^+ to fragmentation from higher levels of the $\tilde{C}$ state. It was not clear how lower parts of the potential surface fragment, but the possibility of decay to $SF_5^+ + F$ has been discussed [11]. Furthermore, the rates of these processes are not known, so it is not known whether the $\tilde{C}$ state is repulsive or supports vibrational levels. SF_3^+ showed thresholds at the adiabatic IPs of the $\tilde{D}$ ^2T_g and $\tilde{E}$ $^2T_{1u}$ states of SF_6^+. As with CF_4^+, due to the lack of electron energy analysis, it was not possible to ascertain whether there were new thresholds for SF_5^+ production at the energies of the higher states of SF_6^+. Furthermore, shape resonances made the observation of such effects very difficult. KE releases in the fragment ions at energies just above their thresholds were difficult to interpret because the internal energy of the SF_6^+ was not uniquely defined.

4. Results

4.1. CF_4

Fig. 1 shows a survey TPES of CF_4 from 15.0 to 23.5 eV recorded at a resolution of 4 Å. This range

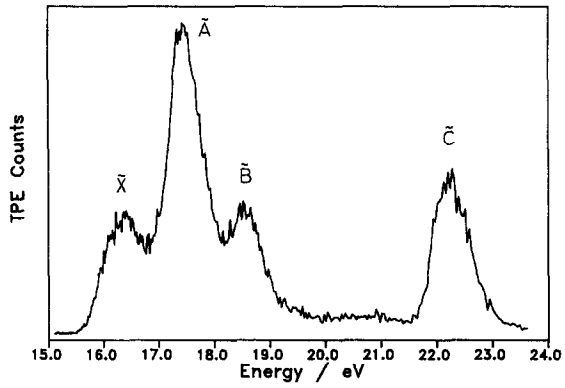

Fig. 1. Threshold photoelectron spectrum of CF_4 recorded at a resolution of 4 Å (120 meV at 19 eV). The spectrum is flux normalised. The electronic states of CF_4^+ are shown.

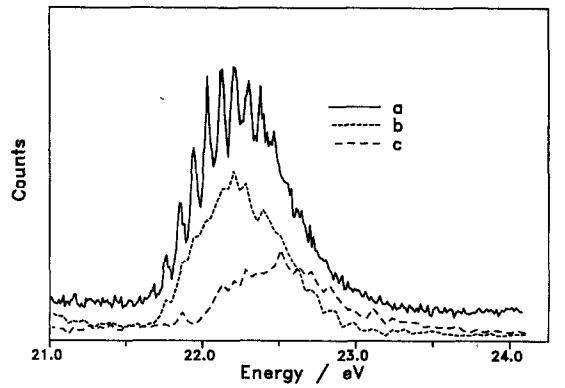

Fig. 2. (a) Threshold photoelectron spectrum of CF_4 between 21 and 24 eV at a resolution of 1 Å (40 meV at 22 eV). (b), (c) Coincidence yields of CF_3^+ and CF_2^+ respectively at a resolution of 2 Å.

spans the ground and first three excited states of CF_4^+. At higher resolution (1 Å) the $\tilde{B}$ band shows a partially resolved progression in ν_1 with only $v_1 = 0$ and 1 clearly resolved, whereas the $\tilde{C}$ state shows a long progression peaking at $v_1 = 5$ (fig. 2a). The survey spectrum is very similar to published He I and II spectra [6,7], showing that resonant autoionisation is not an important process. Our value for the adiabatic IP of the $\tilde{C}$ state (21.67 ± 0.03 eV) is in good agreement with the value determined from the He II PES, and we obtain $\nu_1 = 87 \pm 5$ meV or 702 ± 40 cm^{-1}. This compares favourably with 729 ± 1 cm^{-1} from the CF_4^+ $\tilde{D}$–$\tilde{C}$ high-resolution emission spectrum [24].

TPEPICO spectra in the wavelength-scanning mode were recorded from 14.7 to 24.5 eV at a photon resolution of 2 Å. For energies below 20 eV, CF_3^+ is the only ion observed, and its yield as a function of energy shows an identical shape and structure to that of the TPES (fig. 1) over this range. This is in agreement with earlier studies that the $\tilde{X}$, $\tilde{A}$ and $\tilde{B}$ states of CF_4^+ fragment to $CF_3^+ + F$ [3,20,28]. In our earlier PEPICO study the threshold for CF_2^+ production was observed close to 21.7 eV, the adiabatic IP of CF_4^+ $\tilde{C}\,^2T_2$ [10]. However, the shallow rise in ion yield made it difficult to measure this threshold accurately. In the TPEPICO spectrum coincidences are observed with both CF_3^+ and CF_2^+ between 21.7 and 23.5 eV (the Franck–Condon range of CF_4^+ $\tilde{C}$), and their yields are shown in figs. 2b and 2c. We believe that the predominant cause of the CF_3^+ signal is from radiative decay of the CF_4^+ $\tilde{C}$ state to the repulsive $\tilde{X}$, $\tilde{A}$ states which dissociate directly to $CF_3^+ + F$. As a result the CF_3^+ yield shows a rise and fall which has a similar shape to that of the Franck–Condon determined TPES. As observed before, the rate of rise of the CF_2^+ signal is more gradual, and it is difficult to determine the threshold more accurately than 21.9 ± 0.2 eV. However, it is clear that its yield has a maximum ≈ 0.3 eV to higher energy than that of the CF_3^+ ion. The branching ratio therefore changes when different parts of the CF_4^+ $\tilde{C}$ state potential surface are accessed. This is discussed later.

A wavelength-scanning TPEPICO spectrum was also recorded across the $\tilde{D}\,^2A_1$ state of CF_4^+ from 24.8–26.1 eV at a resolution of 4 Å. Due to the very small partial ionisation cross section into this state [29], extensive signal averaging was necessary. As with the $\tilde{C}\,^2T_2$ state, coincidences are observed with both CF_3^+ and CF_2^+, and fig. 3 shows the threshold electron count and the yields of the two ions as a function of photon energy. (CF^+ is not observed at the $\tilde{D}$ state, contrary to the predictions from measurements of absolute photoionisation cross section by pseudo-photon spectroscopy [30].) At this resolution vibrational structure cannot be resolved in the TPES, but a steep rise at the adiabatic IP (25.04 ± 0.02 eV in our experiment) is observed. The band is substantially broader than the HE II PES [7] (see later). The CF_3^+ signal shows a similar steep rise at threshold, and we believe its predominant cause is

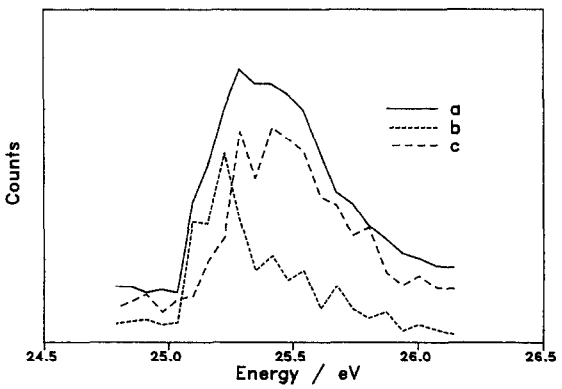

Fig. 3. (a) Threshold photoelectron spectrum of CF_4 between 24.8 and 26.1 eV at a resolution of 4 Å (200 meV at 25 eV). (b), (c) Coincidence yields of CF_3^+ and CF_2^+ respectively at the same resolution.

from radiative decay of the $\tilde{D}$ state to the repulse $\tilde{X}$ and $\tilde{A}$ states. The CF_2^+ signal rises more gradually, and for photon energies greater than 25.25 eV is the dominant ion. Its yield has a maximum ≈ 0.3 eV to higher energy than that of the CF_3^+ ion. As with fragmentation of CF_4^+ $\tilde{C}$, the branching ratio changes when different parts of the $\tilde{D}$ state potential surface are accessed. To quantify this, TPEPICO spectra were recorded at three fixed energies which span the $\tilde{D}$ state. The ratio of the CF_3^+ to CF_2^+ integrated intensity is measured to be 4 ± 1 at 25.12 eV, 0.6 ± 0.2 at 25.33 eV, and 0.15 ± 0.10 at 25.54 eV.

TPEPICO spectra at fixed photon energies were also measured at or close to the Franck–Condon maxima of the five valence states of CF_4^+. Good time resolution (4 ns per channel) was possible for ions resulting from fragmentation of the $\tilde{X}$, $\tilde{A}$, $\tilde{B}$ and $\tilde{C}$ states, but for the $\tilde{D}$ state the resolution had to be degraded to 16 ns. As an example, fig. 4 shows the broadening of the CF_3^+ peak at 22.2 eV, the energy of the Franck–Condon maximum of the $\tilde{C}$ state. Detailed KERDs and hence average energy releases may be derived from an analysis of such TOF peaks [15]. The method used is to compute a set of TOF peaks (each with a discrete energy release ϵ_t) and fit this basis set to the experimental peak using a linear regression technique [15]. The discrete energies are calculated by $\epsilon_t = (2n-1)^2 \Delta E$, where $n = 1, 2, 3, \ldots$ and ΔE (the minimum release when $n = 1$) depends primarily on the statistical quality of the data. In

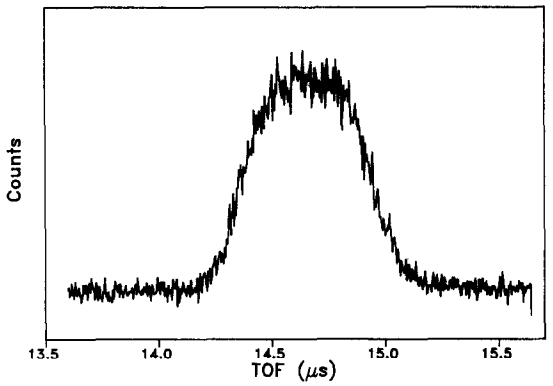

Fig. 4. Coincidence time-of-flight spectrum of CF_3^+ from CF_4 excited at 22.2 eV into the $\tilde{C}\ ^2T_2$ ionic state. The time resolution is 4 ns.

practice we could only reliably obtain average KE releases. The results are shown in table 2, and in each case they are relatively insensitive to the form of the distribution. There are two related reasons why it is not possible to extract a unique distribution from each TOF spectrum. Firstly, the kinematics are unfavourable; in the case of $CF_4^+ \rightarrow CF_3^+ + F$ the daughter ion has over 75% of the mass of the parent. Secondly, the translational temperature T of molecules along the axis of the TPEPICO apparatus is 300 K [2], there being little directionality as the molecules emerge from the inlet needle. With k_BT as high as 25 meV this thermal effect broadens the TOF peak for each value of ϵ_t.

4.2. SF_6

Fig. 5a shows the TPES of SF_6 between 15 and 28 eV recorded at a resolution of 4 Å. The spectrum is very similar to both the He I and II PES [8], showing that resonant autoionisation into states of SF_6^+ in the Franck–Condon gaps is not an important process. TPEPICO spectra in the wavelength-scanning mode were recorded over this energy range at 4 Å resolution. Coincidences are observed with SF_5^+, SF_4^+ and SF_3^+ and their yields are shown in figs. 5b, 5c and 5d, respectively. The threshold for SF_2^+ production (27.0 eV) occurs at the adiabatic IP of the $\tilde{F}\ ^2A_{1g}$ state of SF_6^+ [11], but is very weak due to the low partial ionisation cross section into this state [26]. Since none of the valence states of SF_6^+ decays radiatively [27] these yields must relate to fragmentation of the valence states of SF_6^+. For energies below 18.4 eV, SF_5^+ is the only ion observed and its yield shows an identical pattern to that of the TPES; we conclude that the $\tilde{X}$, $\tilde{A}/\tilde{B}$ and $\tilde{C}$ states of SF_6^+ fragment to $SF_5^+ + F$. There is also a weak contribution to SF_5^+ from the $\tilde{D}$

Table 2
Average KE releases from fragmentation of states of CF_4^+ and SF_6^+

Daughter ion	Parent ion	State	Energy (eV)	$\langle KE \rangle_{trans}$ (eV) [a]
CF_3^+	CF_4^+	$\tilde{X}\ ^2T_1$	16.3	0.97±0.05
CF_3^+	CF_4^+	$\tilde{A}\ ^2T_2$	17.5	1.19±0.04
CF_3^+	CF_4^+	$\tilde{B}\ ^2E$	18.6	1.27±0.14
CF_3^+	CF_4^+	$\tilde{C}\ ^2T_2$	22.2	1.34±0.10
CF_2^+	CF_4^+	$\tilde{C}\ ^2T_2$	22.5	0.57±0.06 [b]
CF_3^+	CF_4^+	$\tilde{D}\ ^2A_1$	25.3	1.54±0.13
CF_2^+	CF_4^+	$\tilde{D}\ ^2A_1$	25.3	1.50±0.26 [b]
SF_5^+	SF_6^+	$\tilde{X}\ ^2T_{1g}$	15.9	0.99±0.02
SF_5^+	SF_6^+	$\tilde{A}/\tilde{B}\ ^2T_{1u}/^2T_{2u}$	17.1	1.21±0.10
SF_5^+	SF_6^+	$\tilde{C}\ ^2E_g$	18.5	1.33±0.09
SF_4^+	SF_6^+	$\tilde{D}\ ^2T_{2g}$	19.8	0.67±0.03 [b]
SF_3^+	SF_6^+	$\tilde{D}\ ^2T_{2g}$	20.0	0.41±0.06 [c]
SF_3^+	SF_6^+	$\tilde{E}\ ^2T_{1u}$	22.5	1.01±0.06 [c]

[a] The quoted error is a measure of how each TOF distribution is fitted, rather than a true representation of the experimental uncertainty.
[b] Assumes the other product is F_2. [c] Assumes the other product is F_3.

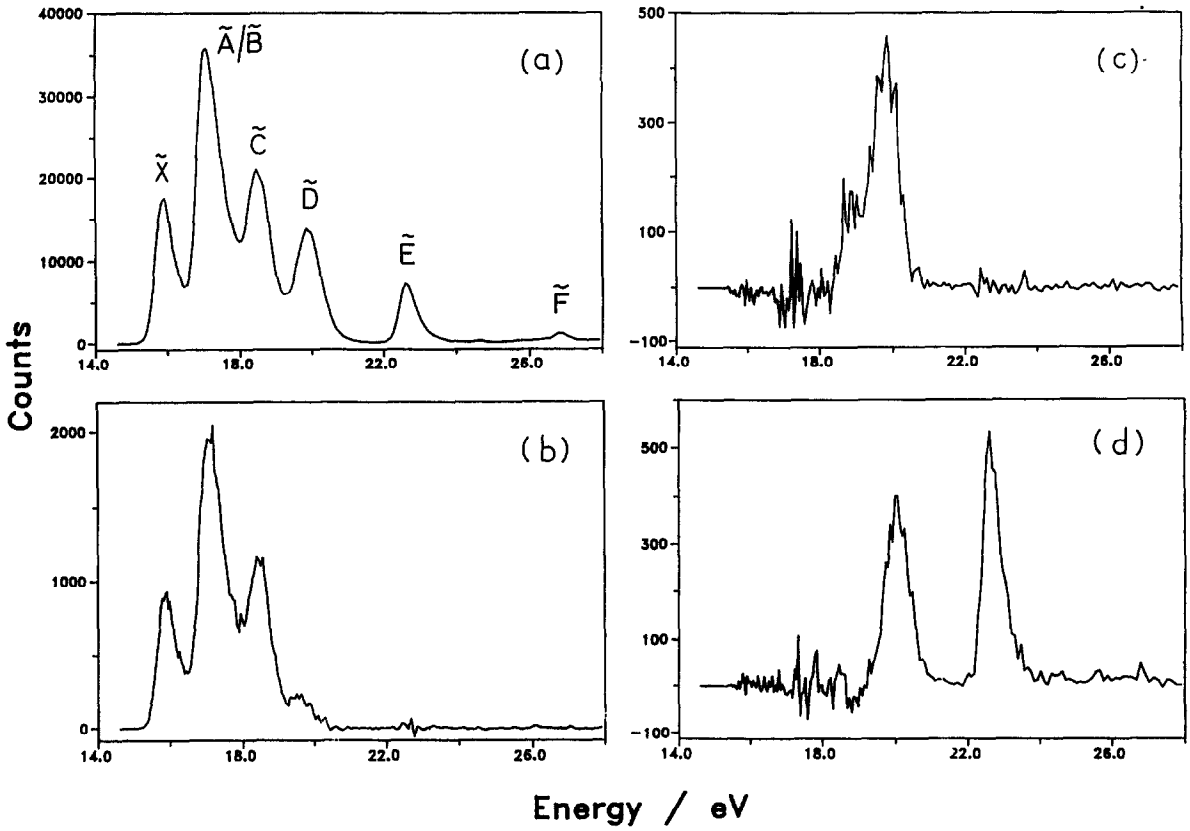

Fig. 5. (a) Threshold photoelectron spectrum of SF_6 between 15 and 28 eV at a resolution of 4 Å. The electronic states of SF_6^+ are shown. (b), (c) and (d) Coincidence yields of SF_5^+, SF_4^+ and SF_3^+, respectively, at the same resolution.

state (fig. 5b). This latter state fragments predominantly to SF_4^+ and SF_3^+ (figs. 5c and 5d), but as before [11] we measure the threshold for SF_4^+ to be 18.4 ± 0.3 eV, which is 0.8 eV lower than the adiabatic IP of the state. This suggests that whilst low vibrational levels of $\tilde{C}$ fragment to $SF_5^+ + F$, higher levels fragment to SF_4^+; the other product(s) could be F_2 or F+F (see later). SF_3^+ shows thresholds at the adiabatic IPs of the $\tilde{D}$ and $\tilde{E}$ states of SF_6^+, as observed previously [11]. TPEPICO spectra at fixed photon energies were measured at or close to the Franck–Condon maxima of the valance states of SF_6^+ which we have studied. As with CF_4^+ only average energy releases could be obtained with confidence, and the results are given in table 2. Note that for $SF_6^+ \rightarrow SF_5^+ + F$ the kinematics are even more unfavourable than in any of the dissociation channels of CF_4^+.

5. Discussion

5.1. CF_4

Our results shows that the $\tilde{X}$, $\tilde{A}$ and $\tilde{B}$ states of CF_4^+ all dissociate to $CF_3^+ + F$, the only ionic dissociation channel open. By analogy with the isoelectronic molecule BF_3, the ground state of CF_3^+ is planar, and therefore a substantial geometry change must occur during the dissociation. Dissociation from the $\tilde{X}$ and $\tilde{A}$ states is direct, whilst that from the $\tilde{B}$ state is almost certainly via internal conversion into the $\tilde{A}$ state. Our results complement those of more conventional PEPICO studies [3,20,28]. We have measured fragmentation of CF_4^+ continuously as a function of energy from below the $\tilde{X}$ state to above the $\tilde{C}$ state, whereas measurements made by other groups were limited to a few specific energies below

that of He I. Our KE releases are in good agreement with others [3,20,28]. For example, our value of 0.97 ± 0.05 eV from CF_4 excited at 16.3 eV into the $\tilde{X}\ ^2T_1$ ionic state can be compared with 0.94 [3] and 1.07 eV [27], and our value of 1.27 ± 0.14 eV from the $\tilde{B}^2E$ state can be compared with 1.12 [3], 1.15 [20] and 1.23 eV [28]. Our result for the $\tilde{X}$ state shows that 61% of the available energy is channelled into translation. This is in good agreement with an impulsive dissociation model assuming a late release of energy, i.e. the dissociation occurs after the CF_3^+ has relaxed to planar geometry [20]. However, this assumes a value of 14.7 eV for the thermochemical energy of $CH_3^+ + F$, and two recent results from ion–molecule studies suggest that this value should be much lower, at around 14.2 eV [5,31]. If this latter value is used then only 46% is channelled into translation. Given the uncertainties in this threshold it is difficult to differentiate between a late and early release model. There is, however, no doubt that dissociation from this state is non-statistical with a large amount of the available energy deposited into translation. The apparent constancy of the mean energy release when different parts of the $\tilde{X}\ ^2T_1$ state potential surface are accessed supports this view [3,20].

The results for the $\tilde{C}\ ^2T_2$ and $\tilde{D}\ ^2A_1$ states of CF_4^+ are new. The former state shows an extensive vibrational progression in ν_1, and the absence of any bands in the degenerate modes ν_2 (e), ν_3 (t_2) and ν_4 (t_2) shows that this state remains tetrahedral, and is not distorted by the Jahn–Teller effect. The state decays radiatively via bound–free $\tilde{C}$–$\tilde{A}$ and $\tilde{C}$–$\tilde{X}$ emission, having a lifetime τ of ≈ 9 ns and a fluorescence quantum yield Φ_F of ≈ 0.5 [17]. The non-radiative channel competing with radiative decay is fragmentation to CF_2^+ [10]. The state-selective nature of our present experiment has allowed us to improve on our earlier data, and we draw the following conclusions:

(a) Assuming that all of the CF_3^+ signal arises from dissociation of the $\tilde{X}$ and $\tilde{A}$ states of CF_4^+ following photon emission from the $\tilde{C}$ state, then at any photon energy the ratio of the CF_3^+ to CF_2^+ signal is the ratio of Φ_F to $(1-\Phi_F)$; Φ_F is defined as $k_r/(k_r+k_{nr})$, where k_r and k_{nr} are rates for radiative and non-radiative decay, respectively. Thus from fig. 2 we see that Φ_F is close to unity for photon energies between 21.7 and 21.9 eV, but decreases thereafter as the energy increases. We obtain $\Phi_F = 0.85$, 0.75, 0.67, 0.52 and 0.33 at energies of 22.0, 22.2, 22.4, 22.6 and 22.8 eV respectively. We conclude that for low vibrational levels of the $\tilde{C}\ ^2T_2$ state radiative decay is the dominant channel, but as higher parts of the $\tilde{C}$ state potential surface are accessed fragmentation to CF_2^+ becomes an increasingly important process.

(b) When integrated over the whole of the $\tilde{C}$ state, the area of the CF_3^+ signal divided by that of the CF_2^+ signal gives the ratio of Φ_F to $(1-\Phi_F)$ for a Franck–Condon weighted average of all vibrational levels of this state. We obtain a CF_3^+ to CF_2^+ ratio of 2.3 to 1, hence $(\Phi_F)_{average} = 0.7 \pm 0.1$. The latter result compares well with values for Φ_F of between 0.5 and 0.6 at photon energies between 23 and 26 eV obtained from non state-selective PEPICO experiments [10]. The former result contrasts with the predicted ratio of the CF_3^+ to CF_2^+ signals of 0.38 to 0.62 obtained by pseudo-photon spectroscopy [30]. The agreement is poor, and furthermore radiative decay was not considered by Zhang et al.; they interpreted the CF_3^+ as arising directly from the $\tilde{C}$ state.

(c) The lifetime data for the $\tilde{C}\ ^2T_2$ state obtained from time-resolved fluorescence measurements [17,32] showed that τ decreases slightly as the photon energy is increased; τ is defined as $(k_r+k_{nr})^{-1}$. The lifetimes measured, however, are not state-selected, but represent an average weighted by Franck–Condon factors of the vibrational levels from threshold up to the photon energy. The true state-selected lifetimes can be measured in a threshold photoelectron–fluorescence coincidence (TPEFCO) experiment [23,33]. Assuming k_r, is constant, we expect τ to fall more rapidly from its threshold value of 9.7 ns than the earlier measurements would suggest [17]. Using the state-selected quantum yields above, we calculate τ to be 8.2, 7.3, 6.5, 5.0 and 3.2 ns at 22.0, 22.2, 22.4, 22.6 and 22.8 eV respectively.

(d) Since fluorescence is observed, fragmentation of the $\tilde{C}$ state of CF_4^+ to CF_2^+ is a relatively slow process. This suggests that the other product is F_2, and not F+F, since the former process involves both the breaking of two bonds and the formation of a new F–F bond. Whilst the $\tilde{C}\ ^2T_2$ state of CF_4^+ does correlate adiabatically to CF_2^+ ($\tilde{X}\ ^2A_1$) + F_2 ($^1\Sigma_g^+$), fragmentation to these two products would involve the formation of a tightly constrained transition state at a barrier along the dissociation coordinate. The average KE release in CF_2^+ cannot be used to distinguish

between these two fragmentation channels. At a photon energy of 22.5 eV, 0.57 eV is released as translational energy, assuming the neutral fragment is F_2 (thermochemical energy = 19.2 eV); this represents 17% of the available energy. If the neutral products are F+F, the total KE release cannot be determined uniquely since this is a three-body fragmentation.

(e) If the CF_3^+ signal arises in part from fragmentation of the $\tilde{C}\ ^2T_2$ state, then the state-selected quantum yields and predicted lifetimes above represent upper limits. However, the similarity of the mean KE release in CF_3^+ from the $\tilde{A}$, $\tilde{B}$ and $\tilde{C}$ states (table 2) suggests that the route for CF_3^+ production is the same for all three states. That is, the $\tilde{B}$ state undergoes internal conversion to the $\tilde{A}$ state, whilst the $\tilde{C}$ state fluoresces predominantly to the $\tilde{A}$ state which subsequently dissociates to $CF_3^+ + F$.

The $\tilde{D}\ ^2A_1$ state of CF_4^+ fluoresces via bound–bound $\tilde{D}$–$\tilde{C}$ [24] and bound–free $\tilde{D}$–$\tilde{A}$, $\tilde{X}$ [25] emission. Its lifetime is 2.1 ns [22]. A TPES of this state recorded recently both at the SuperAco storage ring in Orsay and with the 5 m MacPherson at Daresbury [34] shows an extensive progression in ν_1 with at least six or seven members of comparable intensity. This is very different to the narrow band observed by He II PES [7], and suggests that for this valence state of CF_4^+ resonant autoionisation *is* an important process. As with the $\tilde{C}$ state, the state-selected nature of the present experiment has revealed new aspects of the decay properties of the $\tilde{D}$ state. We draw the following conclusions:

(a) If the same assumptions are made for the origin of the CF_3^+ signal from the $\tilde{D}$ state as from the $\tilde{C}$ state, we obtain values for Φ_F at photon energies of 25.12, 25.33 and 25.54 eV. They are 0.8, 0.4 and 0.1, respectively.

(b) Integrating the CF_3^+ and CF_2^+ signals over the complete $\tilde{D}$ state yields a Franck–Condon weighted average value for Φ_F of 0.3 ± 0.1, consistent with the short lifetime of this state. The value of 2.1 ns was measured by the phase shift method [22], but we have not been able to confirm this, as such a lifetime is too short to be measured reliably by the techniques we employ [17,23]. Using these values, we obtain "averaged" values for k_r and k_{nr} of the $\tilde{D}$ state of 1.4×10^8 and $3.3 \times 10^8\ s^{-1}$, respectively.

(c) The KE release into $CF_3^+ + F$ from the $\tilde{D}$ state is similar to that from the $\tilde{X}$, $\tilde{A}$, $\tilde{B}$ and $\tilde{C}$ states (table 2). We conclude that the predominant route to this ion is via radiative decay. In contrast, the release into $CF_2^+ (+F_2)$ is about three times greater than that from the $\tilde{C}$ state. A possible explanation is that internal conversion occurs into a highly energised region of the $\tilde{C}$ state potential surface prior to dissociation to CF_2^+. A rate of $\approx 3 \times 10^8\ s^{-1}$ is consistent with this model.

5.2. SF_6

The $\tilde{X}$, $\tilde{A}/\tilde{B}$ and $\tilde{C}$ states of SF_6^+ all fragment to $SF_5^+ + F$ with KE releases of 0.99, 1.21 and 1.33 eV, respectively. As with the $\tilde{X}$, $\tilde{A}$ and $\tilde{B}$ states of CF_4^+ fragmenting to $CF_3^+ + F$, these energies do not show the substantial increase which might be expected for non-statistical fragmentation from repulsive parent ion states. For example, the $\tilde{X}$ and $\tilde{C}$ states of SF_6^+ are 3.5 eV apart, yet the KE release into SF_5^+ only increases by 0.34 eV. Internal conversion from the $\tilde{C}$ state may therefore be playing a role. The $\tilde{C}$ state of SF_6^+ also decays to SF_4^+ with a threshold ≈ 0.4 eV above that of the SF_5^+ channel. As with fragmentation of both the $\tilde{C}$ and $\tilde{D}$ states of CF_4^+, the branching ratio changes when different parts of the SF_6^+ $\tilde{C}$ state potential surface are accessed. When integrated over the whole state, however, the ratio of SF_5^+ to SF_4^+ is high, about 8 to 1. Similarly, the $\tilde{D}$ state shows fragmentation into several channels; SF_5^+, SF_4^+ and SF_3^+. In this case the branching ratios favour the highly dissociated fragments, with the ratio $SF_5^+ : SF_4^+ : SF_3^+$ being 1.0:2.0:1.8. The $\tilde{D}$ state shows resolved vibrational structure in photoelectron spectra; its lifetime must therefore be greater than a vibrational period, allowing the possibility of multiple fragmentation channels.

In contrast, the $\tilde{E}$ and $\tilde{F}$ states yield single channels, SF_3^+ and SF_2^+, respectively, and these ions show thresholds at the adiabatic IPs of these states. The SF_2^+ signal is very weak, and is only visible on the colour coincidence map. We are therefore unable to measure a KE release for this ion, but such a measurement would not be meaningful because fragmentation would result in the formation of multiple products (e.g. $SF_2^+ + F_2 + F_2$). The same situation arises with SF_3^+ from the $\tilde{E}$ state, but here the signal is sufficient to measure the KE release. It is clear that the energy release into SF_3^+ from SF_6^+ $\tilde{E}$ is substan-

tially greater than from SF_6^+ $\tilde{D}$ (table 2), but no further quantitative conclusions can be drawn.

6. Conclusions

The results demonstrate that the TPEPICO apparatus can be used to study fragmentation of state-selected polyatomic ions in a way which was not possible with our earlier PEPICO apparatus. We believe that the energy-scanning mode of the TPEPICO experiment is unique, and we are able to record state-selected fragmentation of ions continuously as a function of photon energy. We note that in principle this apparatus can be used to study fragmentation of multiply-ionised species with threshold electron detection; such experiments are planned. The limitations of the present apparatus are twofold. Firstly, the spectral resolution is currently determined by the monochromator, whereas ideally the limitation should be the threshold electron analyser itself. Secondly, the temperature of molecules along the axis of the TPEPICO apparatus is high (300 K). This limits the information that can be obtained from a high-resolution TOF spectrum, especially if the kinematics are unfavourable. Ideally, this apparatus should incorporate a supersonic beam source [35].

For CF_4^+ we have probed in detail the decay properties of all the valence states. The results for the $\tilde{X}$, $\tilde{A}$ and $\tilde{B}$ states confirm earlier measurements, those for the $\tilde{C}$ and $\tilde{D}$ states are new and confirm that radiative decay from these states is an important process. For SF_6^+ we have established fragmentation channels and branching ratios for all the valence states of the ion.

Acknowledgement

We thank the staff at the Daresbury Laboratory (especially Dr. C. Gregory, Dr. A. Hopkirk and Dr. M. Hayes) for help, Dr. M. Stankiewicz for writing the acquisition software, and Mr. K.R. Yoxall for assistance with some of the experiments. We are grateful to Dr. A. Hopkirk and Dr. A. Yencha for communicating their TPES data on the $D\ ^2A_1$ state of CF_4^+ prior to publication. SERC is thanked for an equipment grant, Post-Doctoral Fellowships (PAH and DMS) and a Research Studentship (JCC). BP International plc is also thanked for a Studentship (HMJ). Finally, we thank Mr. M.P. Millard of Reading University for his precise machining of the apparatus.

References

[1] T. Baer, J. Booze and K.M. Weitzel, Vacuum UV photoionisation and photodissociation of molecules and clusters, ed. C.Y. Ng (World Scientific, Singapore, 1991) p. 259.
[2] P.A. Hatherly, M. Stankiewicz, K. Codling, J.C. Creasey, H.M. Jones and R.P. Tuckett, Meas. Sci. Technol. 3 (1992) 891.
[3] I.G. Simm, C.J. Danby, J.H.D. Eland and P.I. Mansell, J. Chem. Soc. Faraday Trans II 72 (1976) 426.
[4] C. Lifshitz and W.A. Chupka, J. Chem. Phys. 47 (1967) 3439.
[5] M. Tichy, G. Javahery, N.D. Twiddy and E.E. Ferguson, Intern. J. Mass Spectry. Ion Processes 79 (1987) 231.
[6] C.R. Brundle, M.B. Robin and H. Basch, J. Chem. Phys. 53 (1970) 2196.
[7] D.R. Lloyd and P.J. Roberts, J. Electron Spectry. Relat. Phenom. 7 (1975) 325.
[8] L. Karlson, L. Mattsson, R. Jadrny, T. Bergman and K. Siegbahn, Physica Scripta 14 (1976) 230.
[9] H.M. Rosenstock, Advan. Mass Spectrom. 4 (1968) 523.
[10] J.C. Creasey, I.R. Lambert, R.P. Tuckett, K. Codling, L.J. Fransinski, P.A. Hatherly, M. Stankiewicz and D.M.P. Holland, J. Chem. Phys. 93 (1990) 3295.
[11] J.C. Creasey, I.R. Lambert, R.P. Tuckett, K. Codling, L.J. Fransinski, P.A. Hatherly and M. Stankiewicz, J. Chem. Soc. Faraday Trans. 87 (1991) 1287.
[12] T. Baer, W.B. Peatman and E.W. Schlag, Chem. Phys. Letters 4 (1969) 243.
R. Spohr, P.M. Guyon, W.A. Chupka and J. Berkowitz, Rev. Sci. Instrum. 42 (1971) 1872.
[13] R.I. Hall, A. McConkey, K. Ellis, G. Dawber, L. Avaldi, M.A. MacDonald and G.C. King, Meas. Sci. Technol. 3 (1992) 316.
[14] W.C. Wiley and I.H. McClaren, Rev. Sci. Instrum. 26 (1955) 1150.
[15] I. Powis, P.I. Mansell and C.J. Danby, Intern. J. Mass Spectry. Ion Phys. 32 (1979) 15.
[16] R.P. Tuckett, Chem. Soc. Rev. 19 (1990) 439.
[17] I.R. Lambert, S.M. Mason, R.P. Tuckett and A. Hopkirk, J. Chem. Phys. 89 (1988) 2683.
[18] K. Codling, J. Chem. Phys. 44 (1966) 4401.
[19] H.A. van Sprang, H.H. Brongersma and F.J. de Heer, Chem. Phys. 35 (1978) 51.
[20] I. Powis, Mol. Phys. 39 (1980) 311.
[21] J.P. Maier and F. Thommen, Chem. Phys. Letters 78 (1981) 54.

[22] J.E. Hesser and K. Dressler, J. Chem. Phys. 47 (1967) 3443.
[23] P.A. Hatherly, K. Codling, D.M. Smith, R.P. Tuckett, K.R. Yoxall and J.F.M. Aarts, Chem. Phys. 174 (1993) 453.
[24] S.M. Mason and R.P. Tuckett, Mol. Phys. 60 (1987) 761.
[25] J.F.M. Aarts, Chem. Phys. Letters 114 (1985) 114.
[26] B.M. Addison-Jones, K.H. Tan, B.W. Yates, J.N. Cutler, G.M. Bancroft and J.S. Tse, J. Electron Spectry. Relat. Phenom. 48 (1989) 155.
[27] T. Field and J.H.D. Eland, Chem. Phys. Letters 197 (1992) 542.
[28] B. Brehm, R. Frey, A. Kustler and J.H.D. Eland, Intern. J. Mass Spectry. Ion Phys. 13 (1974) 251.
[29] T.A. Carlson, A. Fahlman, W.A. Svensson, M.O. Krause, T.A. Whitley, F.A. Grimm, M.N. Piancastelli and J.W. Taylor, J. Chem. Phys. 81 (1984) 3828.
[30] W. Zhang, G. Cooper, T. Ibuki and C.E. Brion, Chem. Phys. 137 (1989) 391.
[31] E.R. Fisher and P.B. Armentrout, Intern. J. Mass Spectry. Ion Processes 101 (1990) R1.
[32] J.C. Creasey, P.A. Hatherly, I.R. Lambert and R.P. Tuckett, Chem. Phys. Letters 188 (1992) 223.
[33] E.W. Schlag, R. Frey, B. Gotchev, W.B. Peatman and H. Pollak, Chem. Phys. Letters 51 (1977) 406.
[34] G. Dujardin, L. Hellner, A. Hopkirk and A. Yencha, unpublished work.
[35] K.M. Weitzel, Chem. Phys. Letters 186 (1991) 490.